Microstructural Investigation of Mudrock Seals Using Nanometer-Scale Resolution Techniques

Amirsaman Rezaeyan[1*], Vitaliy Pipich[2], Pieter Bertier[3], Timo Seemann[4&5], Leon Leu[6], Niko Kampman[7], Artem Feoktystov[2], Lester Barnsley[2], and Andreas Busch[1]

[1]Heriot-Watt University, The Lyell Centre, Research Avenue South, Edinburgh, EH144AP, UK
[2]Forschungszentrum Jülich GmbH, (Jülich Centre for Neutron Science, JCNS) at Heinz Maier-Leibnitz Zentrum (MLZ), Lichtenbergstraße 1, 85748 Garching, GER
[3]RWTH Aachen University, Clay and Interface Mineralogy, Bunsenstr.8, 52072 Aachen, GER
[4]Ghent University, St. Pietersnieuwstraat 33, 9000 Gent, Belgium
[5]Belgian Nuclear Research Centre (SCK-CEN), Boeretang 200, B-2400 Mol, BE
[6]Imperial College London, Department of Earth Science and Engineering, London SW7 2AZ, UK
[7]Shell Global Solutions International B.V., Kessler Park 1, 2288GS Rijswijk, NL

Summary

Small angle neutron scattering (SANS) and nitrogen low-pressure adsorption (LPS) have been used to characterise the pore structure of two organic lean mudrocks, Opalinus Clay, Mont Terri, Switzerland and Carmel Claystone, Utah. This was done in order to obtain a better understanding of H_2 and CO_2 transport, reaction and sorption related to radioactive waste disposal and carbon storage, respectively. The pore structure information derived by SANS and LPS are comparable and the results have revealed a vast heterogeneity from 2 nm to 2 µm, which can be related to the high clay contents. Due to the high clay contents, pores smaller than 10 nm constitute a large fraction of total porosity (25-30 %) and most of specific surface area (up to 80 %) in the sample mudrocks. Accordingly, these interplays contribute to a pore network of few-to-several nano-Darcy permeability in which pore size dependent transport mechanisms can vary from high sorptive diffusional fluid flow in small pores to low sorptive slip flow regime at progressively larger pores.

Introduction

Mudrocks are fine-grained sediments with pore structure that have significantly been altered on different scales due to compaction and diagenesis (Potter *et al.*, 2005). The complexity of pore systems is vast, because a broad range of irregular pore shapes along with a wide distribution of the sizes are entangled with both connected and disconnected pores (Anovitz & Cole, 2015). Permeability and wettability are affected by the pore structure and type, size, and arrangement of pores, controlling fluid transport, storage as well as sealing capacity (Loucks *et al.*, 2012). For these reasons, a quantitative analysis of the pore system is often required as the pore structure and pore connectivity are of major importance in practical applications of mudrocks. According to the IUPAC pore size classification, macropores are >50 nm, mesopores 2-50 nm, and micropores <2 nm in diamater (Rouquerol *et al.*, 1994); pore sizes in mudrocks generally range over several orders of magnitude, i.e., sub-nanometer to several micrometers. Thus, there is no single method that adequately scans this wide range in scale (Busch *et al.*, 2017). Therefore, different methods are often utilised in combination to determine porosity values and to investigate pore structure. The common methods to study pore structure of mudrocks are small angle neutron scattering (SANS) combined with very small angle neutron scattering (VSANS) (Radlinski, 2006) and nitrogen low-pressure adsorption (LPS). These have been employed in this study to provide quantitative structural information with high resolution on two organic lean mudrocks, including Opalinus Clay and Carmel Claystone. Opalinus Clay formation is a potential host rock for deep geological disposal of radioactive waste (Bossart & Thury, 2008) and Carmel Claystone formation acts as seal for CO_2 storage (Kampman *et al.*, 2016).

The main goals of this study are to systematically understand the pore structure of mudrocks with different methods, identify controls on nanoscale pore structure on related pore scale flow processes, and discuss the contribution of nanoscale matrix-related pores to pathways for fluid flow in mudrocks. The results will provide essential input for assessing the feasibility and safety of a deep geological storage/disposal.

Samples and Methods

Experimental work to characterise the pore structure of mudrocks was carried out on two sample sets from different locations, but having almost the same mineralogy and clay content for each set. The similarities in the nature of these mudrocks allows investigating the uniformity of the pore structure. Mineralogical and petrophysical data are provided in Table 1.

1. Opalinus Clay: these samples were obtained from a 10m core section of the shaly facies of the Opalinus Clay formation at the Mont Terri underground rock laboratory, St. Ursanne, Switzerland. The Opalinus Clay was deposited in the Aalenain (Dogger-α, ca. 174 Ma) in a shallow marine setting of an epicontinental sea at water depths of around 10-30 m, and is high in clay content (~70 wt. %), containing mainly illite and kaolinite, and low in quartz (~20 wt. %) and carbonates (~5 wt. %). In Mont Terri, samples are currently at a depth of 230 m but underwent a maximum burial of about 1350 m (Bossart & Thury, 2008).
2. Carmel Claystone: these samples were obtained from a scientific drilling campaign near Green River, Utah, at a burial depth of 200m. The Carmel Formation is a 50 m-thick sequence of complex, laterally gradational lithofacies, comprising interbedded red and grey shale and gypsum, red and grey mudstone/siltstone, and fine grained sandstone. The section analysed is high in clay content (~80 wt. %) containing mainly illite, and low in quartz (~10 wt. %) and carbonates (~7 wt. %). These are interpreted as Mid-Jurassic marine sediments deposited in quiet, subtidal conditions under the influence of periodic hypersaline water and form a regional seal (Blakey *et al.*, 1996).

Table 1 *Sample mineralogy, total organic carbon content (Busch et al., 2017, Kampman et al., 2016), porosity and specific surface area for the sample set used in this study.*

Sample	**Quartz & K-feldespar**	**Carbonate Minerals**	**Clay Minerals**	**TOC**	**Porosity** %		**SSA** m^2/g	
	%	%	%	%	LPS	SANS	LPS	SANS
Opalinus Clay								
CCP01	21.5	4.2	67.7	1.2	NA	20.0	NA	32.9

CCP04	18.3	3.4	72.4	1.0	NA	19.0	NA	33.6
CCP05	18.3	3.5	72.5	1.0	NA	23.0	NA	30.7
CCP06	17.4	3.0	73.6	1.3	NA	17.0	NA	29.5
CCP07	13.9	4.8	76.1	1.5	13.0	25.0	32.2	41.3
CCP09	14.3	4.8	74.0	1.4	13.0	18.0	31.5	30.7
CCP12	13.0	5.5	76.0	1.4	13.0	21.0	30.1	37.1
Carmel Claystone								
NPS095	8.1	7.0	79.9	NA	3.0	6.0	27.3	19.7
NPS089	8.2	7.3	79.2	NA	3.0	5.0	26.2	14.8
NPS086	8.6	7.0	79.6	NA	3.0	6.0	26.7	17.9
NPS080	9.2	7.7	80.7	NA	5.0	5.0	21.5	11.7
NPS077	9.2	8.5	79.4	NA	5.0	6.0	16.7	16.3
NPS073	8.0	5.3	85.7	NA	3.0	4.0	26.7	17.1
NPS069	11.6	2.9	82.0	NA	3.0	4.0	20.8	16.3

In order to characterise the pore structure of the mudrocks studied, SANS and LPS methods were used:

1. Neutron scattering data were collected by two SANS instruments, each of which designed to scan a certain range of pore sizes. This was conducted at the Jülich Centre for Neutron Science (JCNS) outstation at the Heinz Maier-Leibnitz Zentrum (MLZ) in Garching, Germany. The KWS-3 instrument is used to gain VSANS data for pore sizes ranging between ~5 μm and 500 nm (Pipich & Fu, 2015). The KWS-1 instrument provides SANS data representing pore sizes between 500nm and 1nm (Feoktystov *et al.*, 2015). Samples were cut parallel to bedding, fixed on quartz glass carriers, and polished to a thickness of about 200 μm. Samples were dried at room temperature, and measurements performed under ambient pressure and temperature conditions for standard measurements (Busch et al., 2017). Specific surface area (SSA), porosity and pore size distribution (PSD) were calculated from scattering profile (I vs. Q data) by MATSAS for the entire sample set (Rezaeyan *et al.*, 2018).
2. Low pressure N_2 physisorption analysis was performed using the Micromeritics Gemini VII 2390t device to determine SSA, pore size distribution, and porosity. Adsorption and desorption were analysed at relative pressure points in the range of 0.001-0.995 and 0.995-0.1, respectively. Among the parameters calculated from the N_2 adsorption analysis, Brunauer-Emmett-Teller (BET) SSA and Barrett-Joyner-Halenda (BJH) cumulative pore area/volume and pore size distribution (2-100 nm in diameter) were calculated in this study (Bertier *et al.*, 2016).

Results

Clay content of Opalinus Clay samples varies between 67 and 76 wt-%, while the Carmel Claystone has a higher clay content ranging from 79 to 85 wt-% (Table 1). Combined Quartz, K-feldspar and carbonate contents range between 8-22 wt-% and 3-8 wt-%, respectively. Porosity values using SANS range between 0.17-0.25 for Opalinus Clay and 0.04-0.06 for Carmel Claystone, which are higher than the values obtained from LPS. Based on the LPS method, BET SSA of Opalinus Clay samples range from 30.09 to 32.17 m^2/g (average 31.13 m^2/g, Table 1), which is comparable to SANS (average 35.43 m^2/g). BET SSA of Carmel Claystone samples (average 22 m^2/g) are higher than from SANS data (average 15.71 m^2/g, Table 1). Pore size distribution of the two sample sets are illustrated in Figure 1. Differential pore volume distribution of the Opalinus samples are similar for both methods but also for the different samples (Figure 1-A), indicating uniformity of the pore structure of the 10 meter core section analysed as well as comparability of SANS and LPS. The Carmel Claystone sample set features relatively similar differential pore volume distributions at pores <100 Å (Figure 2, left). However, the effect of diagenesis on the pore structure becomes more apparent at pores >100 Å where the sample set reveals different log differential pore volume distribution, resulting from extremely random mineral-mineral interfaces (Figure 1-B).

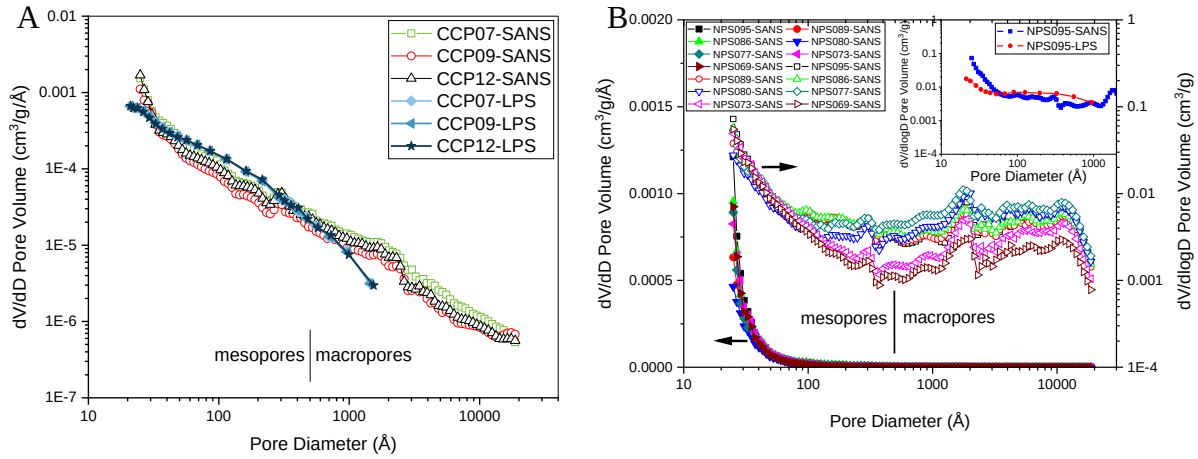

Figure 1 *Pore size distribution of Opalinus Clay obtained with SANS and LPS (A), pore size distribution of Carmel Claystone obtained with SANS with the inset of log PSD by LPS and SANS for NPS095 (B).*

Discussion and Conclusion

The pore size distribution is the relative pore volume associated with different pore sizes, which is essential to determine quantitatively size and number of pores in mudrocks. Fluid transport mechanisms as well as gas or nuclide sorption capacities rely on the average size of pores. For instance, diffusion, slip or continuous flow as well as the modelling thereof depend on pore sizes. Even though porosity might be high, a large fraction of this porosity might be associated with pore sizes where molecule/surface interactions dominate and only diffusional flow or gas slippage is possible. On the other hand, orientation of pores or capillaries for high porosity mudrocks might be random and any directional flux rates will be low. This is important to inform pore network models that aim for an improved understanding of gas or solute transport in mudrocks. By analysing the pore sizes distribution, total porosity and SSA in relation to pore orientation (Leu *et al.*, 2016), we can improve our understanding of these relationships.

Opalinus Clay samples are characterised by a uniform pore network associated with variable pore body sizes from ~2 µm to ~2 nm. Porosity and SSA values obtained by SANS and LPS are comparable. In Opalinus samples, due to the high clay contents, nearly 25 % of the total porosity is associated with pores <10 nm, which provide ~80 % of SSA. On the other hand, macroporosity contributes to more than ~50 % of the total porosity but SSA is about 1 m^2/g. The scale-dependent structural information can be useful to apply different mechanisms at different pore scales. Although additional methods are required to differentiate sorbed phase from free phase, it is clear that the adsorption mechanism needs to be involved in fluid flow equations at pores <10 nm whose SSA of ~26 m^2/g indicates higher gas adsorption capacity compared to Opalinus macropores only providing 3 % of the total SSA. Yet, the high porosity of Opalinus Clay might not improve fluid conductivity since the permeability is controlled by pore throats rather than pore bodies. Derived from random aspect ratios (pore body/pore throat) over the entire pore size scales (Busch et al., 2017), flow in Opalinus Shale is mainly controlled by diffusion for pores <10 nm, followed by slip flow at progressively larger pores.

The Carmel Claystone on the other hand is heterogeneous across pore sizes and SANS and LPS provide different values. This is attributed to pores potentially inaccessible to N_2 but accessible to neutrons. In addition, macropores are covered in LPS to a smaller extend as compared to SANS. Although the purpose of this study is not to compare the pore structure information derived by these two methods, the aim is to provide comparable porosity values with maximum overlap (Clarkson *et al.*, 2012) so that the structural information can be employed in practical models (e.g. pore network modelling). It is of great importance to not only verify models, but also realistically understand fluid flow in the Carmel Claystone formation by defining a well-structured pore network. One of the main criteria to assess the safety of Carmel Claystone formation for CO_2 storage is its pore structure (Kampman et al., 2016). A large fraction of porosity (~30 %) in Carmel Claystone result from pores <10 nm where diffusion (Kampman et al., 2016) is the controlling mechanism. Imaging techniques such as FIB SEM can resolve pores >10nm (Ma *et al.*, 2017) which does not include (most of) pore throats, pores restricting flow to diffusion and adsorption and a large fraction of the porosity. In order to improve pore network/scale

models, the incorporation of SANS PSD, particularly for this pore size range is important to more realistically understand CO_2 (or other gases) migration through mudrock matrix.

Acknowledgements
SANS and VSANS measurements were performed at KWS-1, GP- SANS and KWS-3 instruments of the Jülich Centre for Neutron Science (JCNS) at Heinz Maier-Leibnitz Zentrum (MLZ) in Garching, Germany. We are very grateful for the possibility to conduct measurements at these instruments.

References

Anovitz, L. M. and D. R. Cole, 2015: Characterization and Analysis of Porosity and Pore Structures. *Reviews in Mineralogy and Geochemistry*, **80,** 61-164.

Bertier, P., K. Schweinar, H. Stanjek, A. Ghanizadeh, C. R. Clarkson, A. Busch, N. Kampman, D. Prinz, A. Amann-Hildenbrand, B. M. Krooss, V. Pipich and Z. Di, 2016: On the use and abuse of N2 physisorption for the characterization of the pore structure of shales. *The Clay Minerals Society Workshop Lectures Series.*

Blakey, R. C., K. G. Havholm and L. S. Jones, 1996: Stratigraphic analysis of eolian interactions with marine and fluvial deposits, Middle Jurassic Page Sandstone and Carmel Formation, Colorado Plateau, U.S.A. *Journal of Sedimentary Research*, **66,** 324-342.

Bossart, P. and M. Thury, 2008: Mont Terri Rock Laboratory Project, Programme 1996 to 2007 and Results. *Report of the Swiss Geological Survey.* Wabern, Switzerland.

Busch, A., K. Schweinar, N. Kampman, A. Coorn, V. Pipich, A. Feoktystov, L. Leu, A. Amann-Hildenbrand and P. Bertier, 2017: Determining the porosity of mudrocks using methodological pluralism. *Geological Society, London, Special Publications,* **454**.

Clarkson, C. R., M. Freeman, L. He, M. Agamalian, Y. B. Melnichenko, M. Mastalerz, R. M. Bustin, A. P. RadliÅ„ski and T. P. Blach, 2012: Characterization of tight gas reservoir pore structure using USANS/SANS and gas adsorption analysis. *Fuel*, **95,** 371-385.

Feoktystov, A. V., H. Frielinghaus, Z. Di, S. Jaksch, V. Pipich, M.-S. Appavou, E. Babcock, R. Hanslik, R. Engels, G. Kemmerling, H. Kleines, A. Ioffe, D. Richter and T. Bruckel, 2015: KWS-1 high-resolution small-angle neutron scattering instrument at JCNS: current state. *Journal of Applied Crystallography*, **48,** 61-70.

Kampman, N., A. Busch, P. Bertier, J. Snippe, S. Hangx, V. Pipich, Z. Di, G. Rother, J. F. Harrington, J. P. Evans, A. Maskell, H. J. Chapman and M. J. Bickle, 2016: Observational evidence confirms modelling of the long-term integrity of CO2-reservoir caprocks. *Nature Communications*, **7,** 12268.

Leu, L., A. Georgiadis, M. J. Blunt, A. Busch, P. Bertier, K. Schweinar, M. Liebi, A. Menzel and H. Ott, 2016: Multiscale Description of Shale Pore Systems by Scanning SAXS and WAXS Microscopy. *Energy & Fuels*, **30,** 10282–10297.

Loucks, R. G., R. M. Reed, S. C. Ruppel and U. Hammes, 2012: Spectrum of pore types and networks in mudrocks and a descriptive classification for matrix-related mudrock pores. *AAPG Bulletin*, **96,** 1071-1098.

Ma, L., A.-L. Fauchille, P. J. Dowey, F. Figueroa Pilz, L. Courtois, K. G. Taylor and P. D. Lee, 2017: Correlative multi-scale imaging of shales: a review and future perspectives. *Geological Society, London, Special Publications,* **454**.

Pipich, V. and Z. Fu, 2015: KWS-3: Very small angle scattering diffractometer with focusing mirror. *Journal of large-scale research facilities*, **1**.

Potter, P. E., J. B. Maynard and P. J. Depetris, 2005: *Mud and Mudstones: Introduction and Overview*. Springer, London.

Radlinski, A. P., 2006: Small-Angle Neutron Scattering and the Microstructure of Rocks. *Reviews in Mineralogy and Geochemistry,* **63,** 363-397.

Rezaeyan, A., V. Pipich, P. Bertier, T. Seemann, L. C. Barnsley and A. Busch, 2018: *Small Angle Neutron Scattering in Earth Sciences, Aachen.*

Rouquerol, J., D. Avnir, C. W. Fairbridge, H. J. Everett, H. Haynes, N. Pernicone, J. D. F. Ramsay, K. S. W. Sing and K. K. Unger, 1994: Recommendations for the characterization of porous solids (Technical Report). *Pure and Applied Chemistry,* **66,** 1739–1758.